

The use of Landsat 8 OLI image for the delineation of gossanic ridges in the Red Sea Hills of NE Sudan

Khalid A. Elsayed Zeinelabdein¹, Abdel Halim H. El Nadi²

¹Department of Geology, Faculty of Petroleum and Minerals, Al Neelain University, Khartoum, Sudan

²Department of Geology, Faculty of Science, University of Khartoum, Khartoum, Sudan

Email address

kalsayed2001@yahoo.com (K. A. E. Zeinelabdein), alnadi12@hotmail.com (A. H. El Nadi)

To cite this article

Khalid A. Elsayed Zeinelabdein, Abdel Halim H. El Nadi. The Use of Landsat 8 OLI Image for the Delineation of Gossanic Ridges in the Red Sea Hills of NE Sudan. *American Journal of Earth Sciences*. Vol. 1, No. 3, 2014, pp. 62-67.

Abstract

Gold mineralization type, associated with gossans, was discovered in Ariab area, through the analysis of Landsat images in the nineties of the last century. The main objective of this work is to delineate the gossanic ridges situated NW of Ariab area, which may represent prospective targets for gold mineralization. This can be achieved by applying the spectral band ratioing techniques on Landsat 8 OLI image. Application of the aforementioned techniques revealed characteristic signals of mineral alteration zones (gossanic ridges) that can be accurately mapped and verified by ground checks. XRF analysis of 12 chip samples collected randomly from the gossanic ridges confirmed the presence of gold in the area. Ore microscopic investigation of three samples of sheared gossans provided further evidence of gold mineralization in the study area. The present study demonstrated that the area is economically potential for gold owing to the large tonnage predicted from the delineated target zones.

Keywords

Remote Sensing, Landsat 8, Gossans, Gold Mineralization, Red Sea Hills, Sudan

1. Introduction



Fig. 1. Location map of the study area.

The study area is located in the Red Sea State, about 700 km northeast of Khartoum. It is bounded by latitudes 21° 00' 00.0" and 21° 20' 00.0" N; and longitudes 34° 00' 00.0" and 34° 20' 00.0" E; covering an area of approximately 1350 km² (Fig. 1).

The area is characterized by desert-type climate with hot dry summers and cold dry winters. Temperatures are generally high for most of the year with the highest daily mean reaching 43° in May and June; to less than 20° during winter which extends from December to February. The average annual rainfall is less than 50mm and therefore, the vegetation is scarce and is confined to some of the drainage lines. Topographically, the area is made up of high, linear and sometimes curved ridges of metavolcanics intruded by old and younger granitoids. The former usually form low lying dissected hills, while the latter form much higher dissected granitic massifs reaching up to 100 m above surrounding plane. Several major and minor dry seasonal streams ultimately drain the area in a westward direction. Some of the drainage lines are structurally controlled by

faults and master joints which affect the different geological formations [1].

The Red Sea area is known since old civilizations for its mineral potentialities, particularly the precious metals such as gold which was mined by the ancient Egyptians, the Nubians, the Turkish, British [1] as well as by Sudanese. Gold mineralization type, associated with gossans, was discovered in Ariab Area, southeast of the study area, through the analysis of Landsat images [2] in the nineties of the last century. The study area is characterized by hilly topography and harsh environment which make traditional field survey rather difficult and time consuming. Application of remote sense techniques enables quick delineation of mineralized zones over vast areas at minimum cost and less effort. The present study aims at the demarcation of the gossanic ridges present in the study area which are prospective targets for gold mineralization in the Red Sea Hills of NE Sudan.

2. Tectonic and Geologic Setting

It is now widely accepted that the Arabian-Nubian Shield (ANS) originated and evolved through an ensimatic model, whereby Neo-Proterozoic (900–500 Ma ago) island arcs collided and accreted to the Nile Craton (e.g. [3] – [7]. The contact between the two tectonic domains lies along the Keraf Shear Zone which runs in a N-S direction from Sudanese/Egyptian border to as far south as northern Butana, northeast of Khartoum, e.g. [8], [9]. The accreted island arcs are composed of basic to acid metavolcanics and metasediments and associated I-type granitoids. The different arc assemblages are calc-alkaline demarcated by ophiolitic sequences over shear/subduction zones thus forming five microplates or terranes, e.g. [10], [11]. Flysch-like and molasse-type sediments overlie the greenschist assemblage, the former being in structural concordance with the metavolcanics; while the latter occupied topographic lows [7]. After crust stabilization, post-orogenic, mainly alkaline A-type granitoids intruded the layered sequences mentioned above. Cretaceous sandstones, preserved in places by faults, overlie unconformably the previously mentioned rock groups [1].

3. Methodology

3.1. The Landsat Data Continuity Mission

The Landsat Data Continuity Mission (LDCM) was launched on February 11, 2013 as a joint mission of NASA and the Department of Interior's U.S. Geological Survey [12]. The LDCM satellite payload consists of two science instruments the Operational Land Imager (OLI) and the Thermal Infrared Sensor (TIRS). These two sensors provide seasonal coverage of the global landmass at a spatial resolution of 30 meters (visible, NIR, SWIR); 100 meters (thermal); and 15 meters (panchromatic; Table 1). The LDCM scene size is 185km cross track by 180km along track.

The nominal spacecraft altitude is 705 km. The OLI provides two new spectral bands, one tailored especially for detecting cirrus clouds and the other for coastal zone observations, and the TIRS collects data for two more narrow spectral bands in the thermal region formerly covered by one wide spectral band on Landsats 4–7 [13]. Images of this satellite are coded in 16-bit pixel values.

Table (1). Landsat 8 OLI and TIRS Spectral Bands [13].

Band Number	Spectral Range (µm)	Instrument	Resolution
1	0.43–0.45 (coastal blue)	OLI	30 m
2	0.45–0.51 (blue)	OLI	30 m
3	0.53–0.59 (green)	OLI	30 m
4	0.64–0.67 (red)	OLI	30 m
5	0.85–0.88 (NIR)	OLI	30 m
6	1.57–1.65 (SWIR-1)	OLI	30 m
7	2.11–2.29 (SWIR-2)	OLI	30 m
8	0.50–0.68 (panchromatic)	OLI	15 m
9	1.36–1.38 (cirrus)	OLI	30 m
10	10.60–11.19 (TIR-1)	TIRS	100 m
11	11.50–12.51 (TIR-2)	TIRS	100 m

The spectral bands of Landsat TM are well-suited for recognizing assemblages of alteration minerals (iron oxides, clay, and alunite) that occur in hydrothermally altered rocks [14]. The OLI was designed to detect the same spectral bands as earlier Landsat instruments (i.e., the Thematic Mapper and Enhanced Thematic Mapper Plus sensors) with the exception of the thermal infrared band [13]. Therefore, Landsat 8 OLI image, path 173/raw 45 acquired on 24-04-2013 from the U.S. Geological Survey Earth Explorer was made available for the present study.

3.2. Methods

The best exploration results are obtained by combining geologic and fracture mapping with the recognition of hydrothermally altered rocks [14]. A variety of remote sensing tools is now available to the exploration geologists. The primary task of these tools is to narrow the search area and consequently reduce the duration of the field work and the exploration costs. Accordingly, the present study will rely largely on the interpretation of Landsat 8 OLI image, whereby the gossanic ridges can be accurately mapped utilizing the band ratioing techniques which is capable of emphasizing alteration zones. Band ratioing technique has been proved powerful in discriminating gossan (being rich in iron oxides) from the rest of the country rocks. Geochemical analysis was conducted for a number of samples, collected during the field work, to determine their gold content using portable XRF device.

4. Results and discussions

4.1. Remote Sensing Data Processing and Analysis

The processing of satellite images involved compositing of different images using various band triplets. Standard

colour composites such as 752 in RGB, respectively (Fig. 2) was prepared. The gossanic ridges on this image appear in deep violet color. However, some basic volcanic rock, also, appear in this color making the discrimination of the gossans rather difficult.

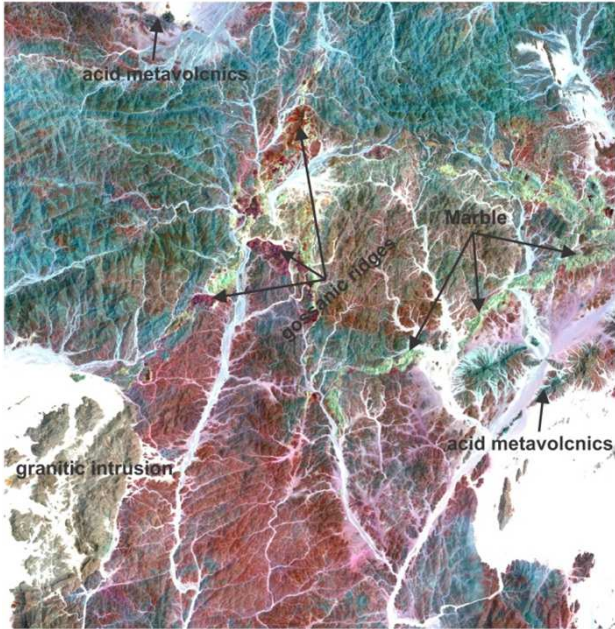


Fig 2. Landsat OLI colour composite image, RGB=753.

Alternative color image of bands 765 in RGB respectively was composed (Fig 3). This image seems to be better in discriminating the gossans which are displayed in dark olive green color. However, as in the previous images, some rocks show the same color as the gossans. This is very clear in the southern part of the image area which is occupied by basic metavolcanic rocks.

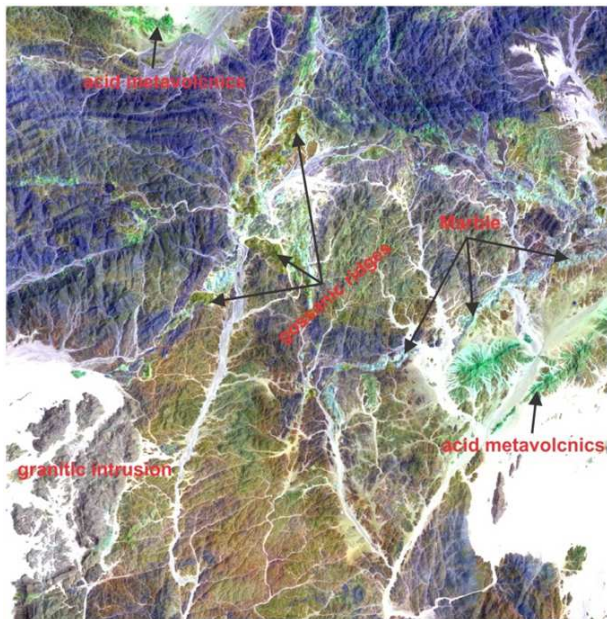


Fig 3. Landsat 8 OLI colour composite image, RGB=765.

In the present study we attempted the application of the band ratioing, a well-known technique of remote sensing in geology. Accordingly, a band ratio colour composite was prepared by assembling the ratios: OLI 6/7, 6/4, 4/2 in RGB, respectively (Fig. 4). As it is clear from this image, the gossans appear in light green hue, but the delineation of these ridges is very difficult, if not impossible. This is because this color is very common in the image and many rock types are displayed in the same color.

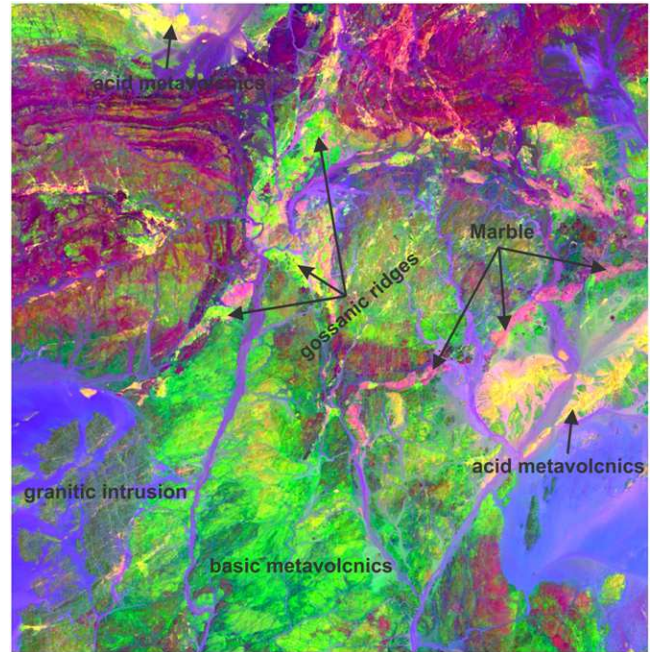


Fig 4. Landsat 8 OLI colour composite of bands ratio: OLI 6/7, 6/4, 4/2 in RGB, respectively.

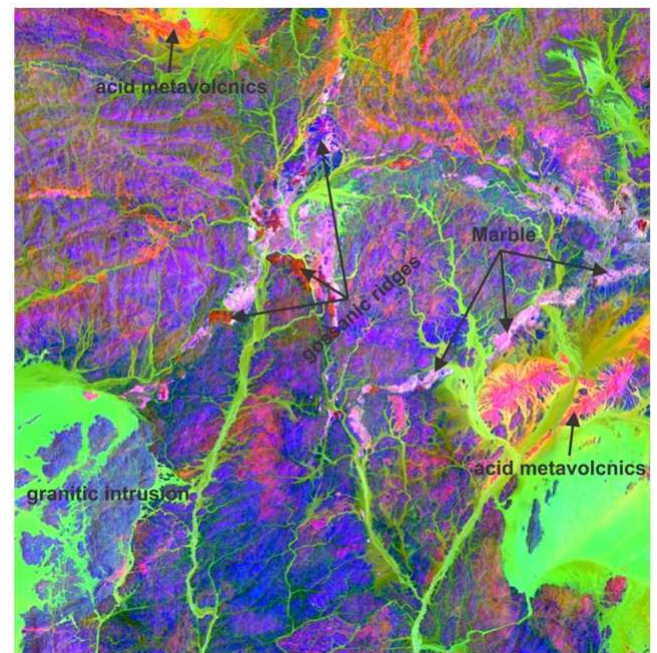


Fig 5. Landsat 8 OLI colour composite of band ratios: 6/7, 4/2, 5/4 in RGB, respectively.

Another band ratio colour composite was prepared by assigning the ratios: OLI 6/7, 4/2, 5/4 to RGB guns, respectively (Fig. 5). On this image the gossans appear in reddish orange to red colors. This color is restricted to the gossanic ridges and no other rock type shares this color. This bands ratio color composite can enable the delineation of the gossanic ridges. Therefore, an on-screen digitizing process was conducted in order to delineate these ridges. The delineated ridges were then superimposed over the Landsat 8 OLI band 7 (Fig. 6).

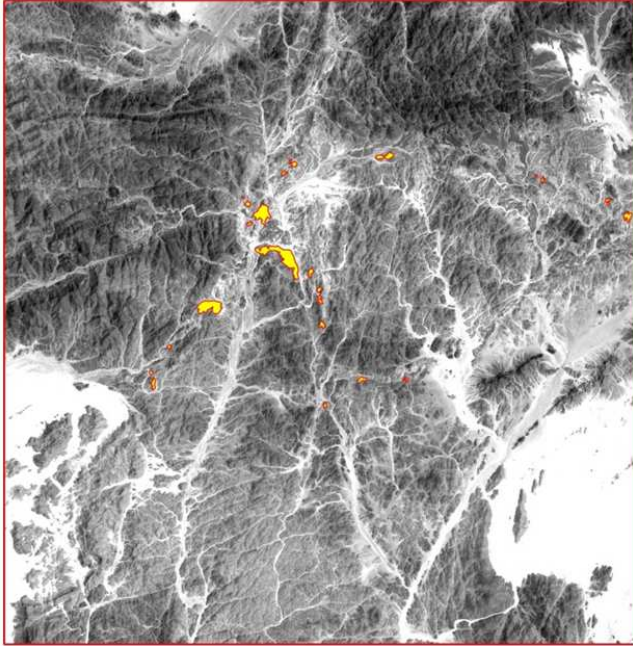


Fig 6. The delineated gossanic ridges underlain by Landsat 8 OLI band 7.



Photo (1). Panoramic view of one of the gossanic ridges in the central part of the study area

Artisans collect gold nuggets from seasonal water courses confirming the presence of gold in the study area (Photo 2).

From Figure (6), it can be observed that the gossanic ridges are found in a close association with the marble. Moreover, they seem to be controlled by certain structural feature. The linearity of the ridges located in western part of the image area can easily be observed and the curvilinear appearance of the ridges in the northern part of the image is not blurred. However, the structural control on the occurrence of these gossanic ridges is beyond the scope of the present study.

4.2. Geochemical Analysis

Based on the results of OLI image interpretation, 9 ore samples were selected for XRF analysis from the delineated gossanic ridges (Fig. 6, photo 1). The obtained results are displayed in Table (2). However, more accurate analytical techniques (e.g. Inductively Coupled Plasma ICP, Atomic Absorption Spectrometry AAS) are recommended.

Table 2. Gold content in part per million (ppm) for selected samples.

Sample No.	Au content (ppm)	Sample No.	Au content (ppm)
H_12	13.3	H_35-B	7.9
H_25	22.5	H_36	6.4
H_26	30.2	H_41	17.3
H_27	1.8	H_46	1.4
H_35	16.2		



Photo (2). Gold nuggets collected by the Artisans from the study area.

4.3. Ore Microscopy

The study of polished sections from two gossanic outcrops (namely: H_26 and H_12) proved the gossanic nature of the ridges and the presence of gold (Plates 1 and 2). The gold grains depicted in the microphotographs are very small, attributed to the rejuvenation of shearing [1].

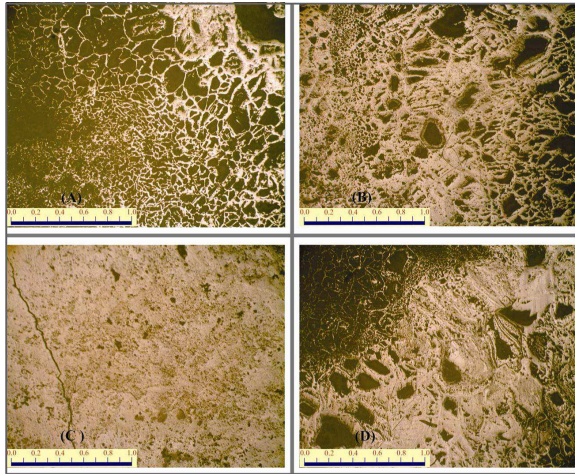


Plate 1. Photomicrographs from locality H_26. A and B show the boxworks structure typical of gossans. The minerals composition includes: magnetite (whitish), hematite (brownish) and secondary limonite. Ilmenite appears as streaky form and pyrite as dark cubic crystals in C and D.

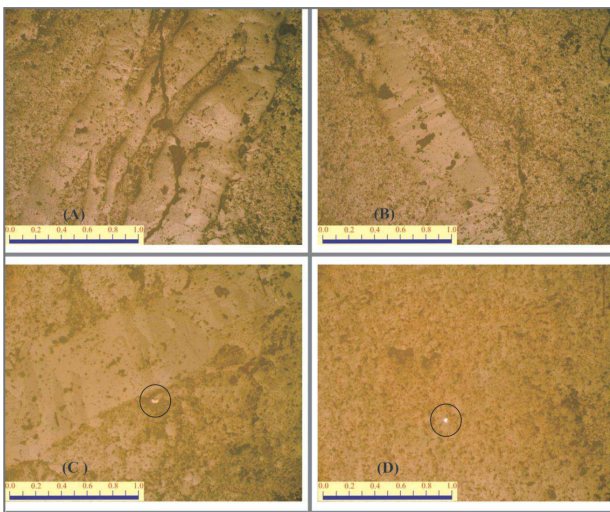


Plate 2. Photomicrographs from locality H_12. A and B show magnetite (whitish) and haematite (later crystallization, pale brown in colour) as veinlets. Gold grains are seen in C and D as the brightest grains. Dark cubes of pyrite appear in D.

5. Conclusions

The geology of the study area comprises rocks of greenschist facies (basic to acid metavolcanics), subordinate metasediments and the associated gossanic ridges. These rocks are intruded by older and younger granitoids.

Digital image processing revealed areas with favourable hydrothermal alteration signals that were later verified in the field. Geochemical analyses using portable XRF device revealed the presence of gold in the area. Further evidence of gold mineralization in the study area is provided by the study of polished sections from the identified gossans.

The outcome of the present study indicated high potentiality for gold in the area. However, further detailed studies are needed in order to quantitatively evaluate the gold reserves in the study area.

Acknowledgments

The authors would like to thank Mr. Adli Abdelmageed for the geochemical analysis and continuous encouragement. Thanks are extended to the geologist Asim Abdalaziz Abdelrahman for his considerable help during the field work and the samples analyses in Sudan. The work of Dr. Samia Abdelrahman of Geology Department, University of Khartoum on the polished sections is gratefully appreciated. Special thanks are due to Dr. Ali Eisawi of Al Neelain University for fruitful discussions and valuable comments. Thanks are due to the editor and anonymous reviewer.

References

- [1] A.H. El Nadi and K.A. Elsayed Zeinelabdein. Geological report on the gold mineralization east of Wadi Gabgaba, northeastern Sudan. Unpub. report, 2011.
- [2] K.A. Elsayed Zeinelabdein. Sudan experience in using remote sensing for mineral prospecting. Proceedings of the 11th Arab International Conference on Mineral Resources, Arab Industrial Development and Mining Organization, Tripoli, Great Jamahiriya. p. 636-644, Oct. 25-27 2010.
- [3] W.R. Greenwood, D.G. Hadley, R.E. Anderson, R.J. Fleck and D.L. Schmidt. Late Proterozoic cratonization in southwestern Saudi Arabia. Phil. Trans. R. Soc. Lond. A, 280, 517-527, 1976.
- [4] I.G. Gass. The evolution of the Pan African crystalline basement in NE Africa and Arabia. J. Geol. Soc. Lond., 134, 129-138, 1977.
- [5] A. Kröner. Pan African plate tectonics and its reconstructions on the crust of north-east Africa. Geol. Rundsch. 68, 565-583, 1979.
- [6] A.H. El Nadi. The Geology of the Late Precambrian Meta-volcanics, Red Sea Hills, northeast Sudan. Ph.D. thesis, Nottingham University. 284 pp., 1984.
- [7] A.H. El Nadi. Late Precambrian volcanism in NE Sudan and the evolution of the Nubian Shield. Journal of the African Earth Sciences, Pergamon Press, London; Vol. 9, No. 3/4, 467-480, 1989.

- [8] D.C. Almond and F. Ahmed. Ductile shear zones in the northern Red Sea Hills, Sudan, and their implication for crustal collision. *Geol. J.*, 22: 175-184, 1987.
- [9] A. Kröner, D. Linnebacher, R.J. Stern, T. Reichmann, Manton, and I.M. Hussein. Evolution of Pan African island arc assemblages in the southern Red Sea Hills, Sudan and southwestern Arabia as exemplified by geochemistry and geochronology. *Precamb. Res.* 53: 99-118, 1991.
- [10] D.B. Stoeser and J.S. Stacey. Evolution, U-Pb geochronology, and isotope geology of the Pan-African Nabitah orogenic belt of the Saudi Arabian Shield. In: *The Pan-African belts of northeast Africa and Adjacent areas* (Edited by El Gaby, S. and Greiling, R. O.) pp227- 288. Friedr Vieweg and Sohn, 1988.
- [11] M.G. Abdelsalam and R.J. Stern. Tectonic evolution of the Nakasib suture, Red Sea Hills, Sudan: evidence for a late Precambrian Wilson Cycle. *J. Geol. Soc. London*, Vol. 150: 393-404, 1993.
- [12] LDCM Landsat Data Continuity Mission. 29th Annual Louisiana RS/GIS Workshop. April 23, Cajundome Convention Center, Lafayette, Louisiana, 2013.
- [13] <http://www.nasa.gov>, accessed 25 June 2013.
- [14] Sabins, F.F. (1999). Remote sensing for mineral exploration. *Ore Geology Reviews* 14: 157–183.